

Design and evaluation of a probe for simultaneous EEG and near-infrared imaging of cortical activation

R J Cooper¹, N L Everdell¹, L C Enfield¹, A P Gibson¹, Alan Worley²
and Jeremy C Hebden¹

¹ Department of Medical Physics & Bioengineering, University College London, Gower Street, London WC1E 6BT, UK

² Clinical Neurophysiology, Great Ormond Street Hospital, London WC1N 3JH, UK

Received 12 January 2009

Published 12 March 2009

Online at stacks.iop.org/PMB/54/2093

Abstract

We present a novel probe design which enables simultaneous electroencephalography (EEG) and near-infrared (NIR) optical imaging to be performed in a manner which is easy to apply, allows for optimum co-registration of the two forms of data and maximizes the number of sensors which can be applied to a given area. Our probe design is evaluated using a dual-modality, tissue-mimicking phantom and by performing a simple functional activation study of the human motor cortex. We successfully acquired NIR optical and EEG data simultaneously for both our phantom and our human motor cortex experiments, clearly demonstrating the effectiveness and suitability of our ‘opto-electrode’.

1. Introduction

Near-infrared (NIR) imaging techniques are a versatile and increasingly popular means of studying blood flow and oxygenation in human tissue (Gibson *et al* 2005, Hillman 2007). They exploit the significant differences in the absorption spectra of the oxygenated and de-oxygenated forms of haemoglobin at near-infrared wavelengths. By measuring the changes in the intensity of diffusely transmitted near-infrared light across a region of tissue it is possible to gain well-localized information about blood oxygenation and haemodynamics. Optical topography (OT) is the application of NIR techniques to produce spatially resolved, two-dimensional images of changes in both oxyhaemoglobin (HbO₂) and de-oxyhaemoglobin (HHb) (Obrig and Villringer 2003). Optical topography is most commonly used to observe the haemodynamic response of surface areas of the brain to a chosen stimulus. OT has been used extensively to study the functional activation of the motor (Franceschini *et al* 2003, Maki *et al* 1996) and visual (Zeff *et al* 2007) cortices as well as being used in the studies of language processing and development (Peña *et al* 2003).

The most commonly used systems for the study of functional activation can be broadly grouped into two types: those which directly measure the electromagnetic effects of activation of groups of neurons (electroencephalography (EEG) and magneto-encephalography) and those which measure the subsequent vascular response to this activation (functional magnetic resonance imaging, positron emission tomography and NIR imaging). EEG is a widely practiced technique for measuring the variations in electrical potential across the scalp surface. Typically, chlorided-silver or gold-plated electrodes are coupled directly to the head using a conductive paste or gel, and the often noisy signal is carefully amplified and filtered using increasingly sophisticated methods (Nuwer 1997).

The electrical signal monitored by EEG is a superposition of all underlying neuronal electrochemical activity and consequently is very difficult to localize (Michel *et al* 2004). For this reason, and because of the presence of the skull, cerebrospinal fluid and other layers of tissue between the cortex and an electrode, EEG spatial resolution is typically very low. The great advantage of EEG, however, is its high temporal resolution, which allows sub-millisecond signal variation to be observed.

The study of functional activation using EEG is also well established. The relatively low signal-to-noise ratio of the electrophysiological response to activation (known as an event-related potential, ERP) requires that the stimulus be repeated many times during EEG recording and a system of block averaging be applied in order that a well-defined event-related potential can be observed. ERP experiments have been performed extensively in the study of all aspects of human cortical function, including visual attention (Hillyard and Anllo-Vento 1998, Gonzalez *et al* 1994), language development and impairment (Connolly *et al* 2000) and movement (Babiloni *et al* 1999, Mima *et al* 1999).

The relationship between neuronal activity in the cerebral cortex and the resulting haemodynamic response (known as neurovascular coupling), is not well understood and is the subject of ongoing research (Shibasaki 2008). It is, however, beyond doubt that there is a strong correlation between mass neuronal activity and localized changes in cortical blood flow, and any system which observes both simultaneously is of benefit to investigations of functional cortical activity and of neurovascular coupling itself. The complementary information that can be gained by simultaneously measuring electrophysiological changes at the scalp and changes in cerebral blood volume has been exploited by simultaneous recording of EEG and fMRI (Ritter and Villringer 2006, Mulert *et al* 2004), and more recently by simultaneous EEG and NIR spectroscopy (Rovati *et al* 2007, Roche-Labarbe *et al* 2007).

Previous attempts to combine EEG with NIR imaging have involved attaching separate arrays of electrodes and optical fibres ('optodes') to the subject's head and have therefore been unable to perform optical topography and multi-channel EEG over the same cortical area. In this paper, we present a design of probe which integrates optodes and electrodes and thereby maximizes the ease of application and also maximizes the number of sensors which can be applied to a given area of the scalp. The following section describes and justifies our design of a combined modality head probe and section 3 includes a description of a dynamic dual-modality phantom which we have designed to evaluate it. The results of this evaluation and of a preliminary case study of adult motor activation observed by simultaneous ERP and NIR imaging are described in sections 3 and 4, respectively.

2. Methods

2.1. Opto-electrode probe

To facilitate simultaneous attachment of many electrodes and optodes to a subject's scalp we have developed a novel 'opto-electrode' which houses both an EEG electrode and an optical

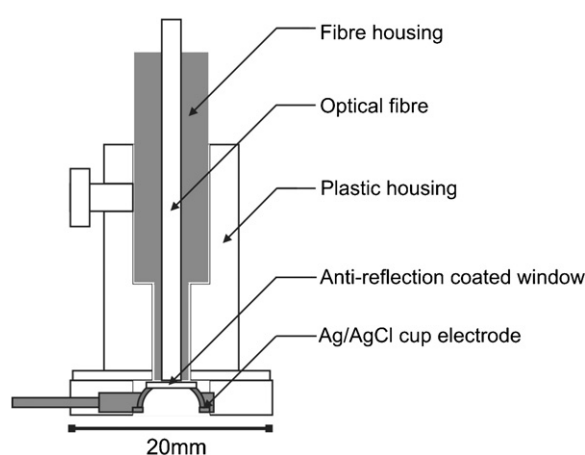


Figure 1. A schematic diagram of the opto-electrode.

fibre bundle, as shown in figure 1. The base of a clinical standard Ag–AgCl cup electrode (Micromed Electronics Ltd, Italy) is replaced with a 0.5 mm thick window of anti-reflection coated polycarbonate (VisionTek Systems Ltd, UK), which has an optical transmission of approximately 92% at 800 nm. The electrode cup and window are then located directly beneath the end of an optical fibre bundle. When used *in vivo*, an electrode coupling gel with low optical absorbance and negligible scattering at NIR wavelengths is applied to the lower surface of the electrode cup to minimize the impedance of the electrode–skin interface, as is common practice in clinical EEG.

This design of opto-electrode has the significant advantage of maximizing the number of electrical and optical sensors possible to apply to a given area, which is of particular importance when studying neonatal brain function. The probe design allows for fast and simple application and co-locates the optical source or detector with the electrode to allow for optimal co-registration of the two forms of measurement.

2.2. Optical Imaging

The optical topography system developed at University College London (Everdell *et al* 2005) can employ up to 32 laser diode sources (16 at 770 nm and 16 at 850 nm) and 16 avalanche photodiode detectors. Sources are arranged in pairs, with each pair consisting of one 770 nm source and one 850 nm source. All sources are illuminated simultaneously, with each modulated at a different frequency. A Fourier transform of the diffusely reflected intensity measured at each detector thus allows the contribution from each source to be isolated. The considerable flexibility of the UCL OT system allows for any arbitrary source-detector arrangement to be used within the limiting separation of approximately 40 mm.

Optical images are reconstructed using a linear image reconstruction algorithm based on the Rytov approximation (Gibson *et al* 2006). An image of the change in optical absorption is computed using the difference in log-amplitude intensity recorded across each source–detector pair between a sample data set and a reference data set. Reconstructing an image from our data requires a solution to the inverse problem represented by the matrix equation $\Delta y = J\Delta x$, where Δy is the difference between log amplitudes of sample and reference data, Δx are the corresponding changes in optical absorption, and J is the Jacobian or sensitivity matrix.

For the images presented here, the Jacobian was calculated using the TOAST software package and assuming uniform optical properties ($\mu'_s = 1.0 \text{ mm}^{-1}$ and $\mu_a = 0.01 \text{ mm}^{-1}$) in order to solve the diffusion equation using the finite element method (Arridge 1999). An image representing the 3D distribution of the change in optical absorption is then generated by inverting the Jacobian. This is achieved using Tikhonov regularization of the Moore–Penrose generalized inverse $\Delta x = J^T (JJ^T + \lambda I)^{-1} \Delta y$, where the regularization parameter λ was set between 1 and 5% of the largest singular value of JJ^T , and where I is the identity matrix. Note that the accuracy of the amplitude of reconstructed changes in optical absorption is severely limited by its strong dependence on the choice of regularization parameter.

2.3. EEG Recording

For our phantom study, a Grass-Telefactor H₂O 32-channel EEG recording system (Grass Technologies, Astro-Med Inc.) with a sample rate of 400 Hz and a PC interface were used to acquire and amplify the EEG signals. Data were acquired using the software package EEG TWin 2.6 (Grass Technologies, Astro-Med Inc.), and were recorded over the range 1–70 Hz. For our motor cortex study we used a Neuroscan Synamps 32-channel EEG/ERP system with a sample rate of 2000 Hz, linked to the Scan 4.2 data acquisition package (Compumedics Ltd, USA). Data were recorded over the range 0.1–70 Hz with a 50 Hz notch filter.

3. Dual modality phantom

To assess the ability of our probe design to acquire simultaneous OT and EEG data, a dual modality phantom was built which provides both optical and an electro-potential contrast. The phantom is shown in figure 2. It consists of a solution of 1% Intralipid[®] emulsion (Flock *et al* 1992) with a tissue-like transport scattering coefficient (μ'_s) of 1.0 mm^{-1} , and an NIR-absorbing dye (S109564, ICI Ltd) which provides an absorption coefficient (μ_a) of 0.01 mm^{-1} at wavelengths around 800 nm. Sodium chloride was added to this solution at 0.2% concentration in order that the liquid phantom had similar conductive properties to brain tissue (Tidswell *et al* 2001). The solution was contained within an HDPE tank of approximate dimensions $160 \text{ mm} \times 240 \text{ mm} \times 120 \text{ mm}$.

To provide a region of both optical and electrical contrasts within the Intralipid solution a polyester resin cylinder (radius 10 mm and length 20 mm) was constructed with the same scattering properties as the solution ($\mu'_s = 1.0 \text{ mm}^{-1}$) but higher NIR absorption ($\mu_a = 0.04 \text{ mm}^{-1}$ at 800 nm). A current dipole was then embedded centrally within the cylinder, formed from two Ag–AgCl pellet electrodes, 2 mm in length, set 5.5 mm apart. The cylinder was attached to an insulated arm supported by a three-axis micrometer stage so that it could be positioned anywhere within the tank. The pellet electrodes were coupled to the positive and common terminals of an 11 Hz sine-wave signal generator which produced a current-dipole moment of the order of $10 \mu\text{A mm}$. Such a current-dipole moment was found to provide a maximum potential difference across electrodes of around $20 \mu\text{V}$, comparable to those measured across the scalp during EEG.

A $30 \text{ mm} \times 90 \text{ mm}$ opto-electrode array consisting of eight opto-electrodes in a 2×4 grid arrangement was constructed and connected to four dual-wavelength sources and four detectors. This array provided ten source–detector pairs (per wavelength) of a suitable separation and is shown in figure 3(a). The array was suspended over the centre of the tank at the surface of the phantom solution such that all electrodes were submerged and no air gaps existed between the surface of the solution and the polycarbonate window.

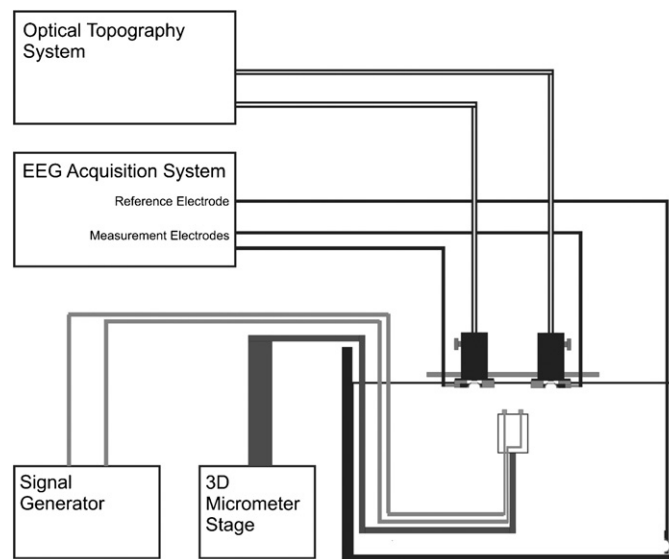


Figure 2. The dual-modality liquid phantom.

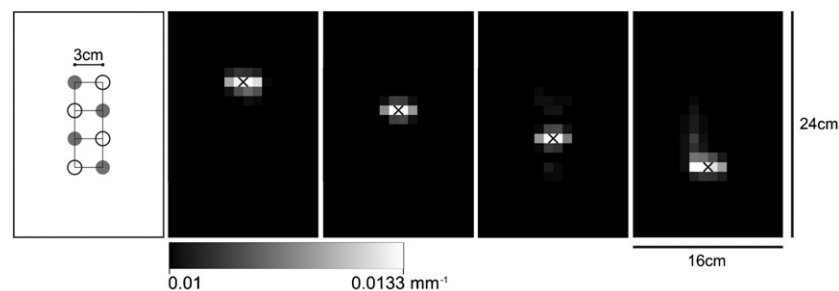


Figure 3. (a) The phantom probe array. Filled circles correspond to sources and open circles to detectors, whilst each line indicates a viable source–detector pair; (b) to (e) show the reconstructed images of changes in optical absorption at 850 nm scaled to the maximum range of 0.01–0.0133 mm⁻¹. The black cross in each indicates the actual position of the target.

3.1. Phantom results

The cylindrical target/current dipole was positioned such that the cylinder was at a suitable depth to be observed by optical topography, extending from approximately 4–24 mm below the surface. This placed the top of the current dipole at a depth of 2 mm below the surface. The target was then translated along a path bisecting the short axis of the array in steps of 5 mm. Ten second long sets of optical topography and EEG data were recorded at each position. An additional set of OT data was also recorded with the target absent from the tank in order to provide a reference for image reconstruction.

The signal from each EEG channel was recorded relative to a common reference electrode positioned in the bottom corner of the phantom tank (see figure 2). The impedance of each channel was recorded at the start of the experiment and all were below 1 k Ω .

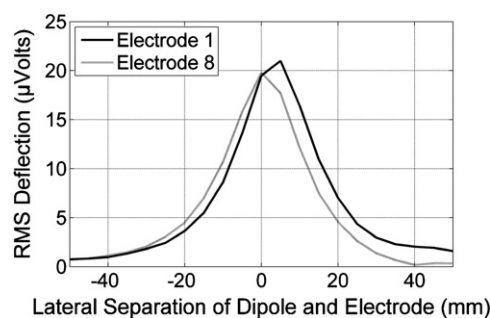


Figure 4. The 10–12 Hz band-passed RMS deflection recorded at the uppermost pair of electrodes for varying lateral separation of dipole and electrodes.

Figures 3(b)–(e) show four reconstructed images of the change in optical absorption as the cylindrical target is moved centrally down the long axis of the array, at a depth averaged between 10 and 20 mm. As is clearly apparent, the correspondence between the positions of peak change in absorption measured by optical topography and the actual target position is very good. The mean two-dimensional error between the centre of the reconstructed peak absorbance change and the actual target centre is 3.8 mm.

Figure 4 shows the band-passed RMS voltage recorded at the upper pair of electrodes (electrodes 1 and 5) as the dipole target passed beneath them. These data are typical of that measured at each of the eight electrodes. The peak RMS electrical potential difference measured by the EEG array also shows good one-dimensional localization of the target, which one would expect in a homogeneous conducting medium. The mean one-dimensional error between the position of peak RMS electrical potential difference and actual target position is approximately 1.3 mm.

The image shown in figure 3(b) was reconstructed from data acquired when the target was closest to the upper pair of electrodes. Figure 3(b) therefore corresponds to the position of 0 mm lateral separation in the EEG data shown in figure 4.

4. Functional activation of the motor cortex

In order to further assess the suitability of our probe design for simultaneous optical imaging and EEG of cortical activation we devised a simple motor cortex stimulation paradigm which would provide an event-related electrophysiological response and a vascular response both significant enough to be observed in a single-subject trial.

Because of the vastly different timescales of most functional haemodynamic responses (peaking of the order 10 s post-stimulus) and ERPs (of the order 100 ms post-stimulus) it was necessary to split the stimulus paradigm into two parts. The first consisted of 15, 30 s long, continuous, self-paced finger-to-thumb opposition movements with the dominant hand, followed and preceded by 30 s of rest. These events were time-locked to the optical topography recording using a control PC running the Cogent 2000 software toolbox (Institute for Cognitive Neuroscience and Functional Imaging Laboratory, UCL) within Matlab (Mathworks Inc.). The second part consisted of 15 min of recording whilst the subject responded to a 0.2 Hz metronome by raising the forefinger of their dominant hand. This movement was time-locked to the EEG trace using a simple optical break-beam trigger. Simultaneous EEG and OT recording occurred continuously throughout both parts of the experiment.

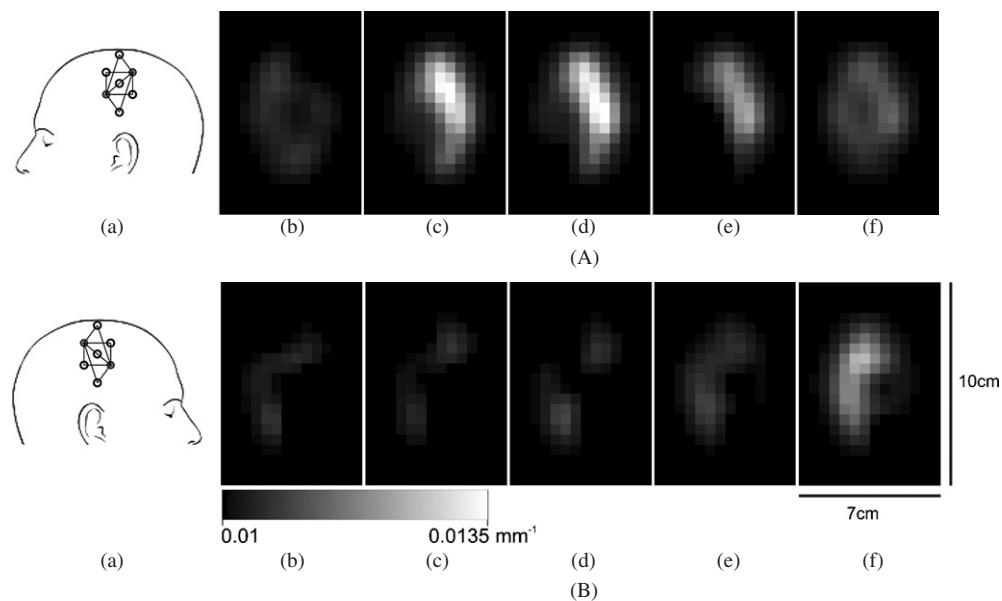


Figure 5. Panels A(a) and B(a) show the approximate positions of the opto-electrode arrays over the left (contralateral to movement) and right (ipsilateral to movement) motor cortices, respectively. Filled circles correspond to sources and open circles to detectors, whilst each line indicates a viable source–detector pair. Panels A(b–f) and B(b–f) show the reconstructed images of mean changes in optical absorption at 770 nm for the time windows 5–10, 10–15, 15–20, 20–25 and 25–30 s post-movement onset for the left and right motor cortices respectively at a depth of 10–15 mm. All are scaled to the maximum range across all ten images, 0.01–0.0135 mm^{-1} .

The first part of the experiment is designed to provide a large enough stimulation of the motor cortex to observe a vascular response using the optical topography system. The continuous finger-to-thumb opposition task has previously been shown to produce a significant haemodynamic response in the contralateral motor cortex in a good proportion of subjects (Franceschini *et al* 2003, Everdell *et al* 2005).

The aim of the second part of the experiment was to observe a ‘Bereitschaftspotential’ (BP) or ‘readiness potential’ within the EEG recording. A BP is an electrophysiological sign of the activation of the supplementary motor area of the motor cortex prior to voluntary movement (Shibasaki and Hallett 2006). The Bereitschaftspotential is often separated into two parts: early BP, which consists of a slow negative deflection from -2 to -0.5 s post-movement and a late BP which is a further decrease at a greater rate observed from -0.5 to 0 s post-movement. Early BP tends to be observed bilaterally whilst late BP tends to be well localized over the motor cortex contralateral to movement.

The eight opto-electrode array design used in the phantom study was modified to hold seven opto-electrodes (two acting as dual-wavelength sources and five as detectors, and all seven as sensing electrodes) such that eight viable optical channels per wavelength were arranged over an area of less than $30 \text{ mm} \times 65 \text{ mm}$. Two of these arrays were produced to be placed symmetrically over both the left and right motor cortices such that the central opto-electrodes were located at C3 and C4 respectively, using the international 10–20 system. The arrays are shown in figures 5A(a) and B(a) in their approximate positions on the head.

4.1. Motor cortex study results

The subject was a healthy, right handed, 24 year-old male volunteer. The opto-electrode contact sites were abraded prior to the study using an abrasive paste in order to remove excess dead skin which can limit the quality of electrical contact. The contact impedance of each channel was measured before the beginning of the paradigm and kept below 5 k Ω . Note that a good electrical and a good optical contact were achieved despite the subject having a full, albeit short, head of hair.

The two opto-electrode arrays were linked together over the top of the head and then secured using light bandaging. A ground electrode was placed at Cz and a common reference electrode was placed on the tip of the nose. The subject was instructed to keep his eyes closed for the second part of the experiment in order to minimize eye-movement artefacts on the EEG trace.

Figures 5A(b–f) show changes in optical absorption over the left (contralateral to movement) motor cortex with time at a depth averaged between 10 and 15 mm, whilst figures 5B(b–f) show the corresponding changes over the right (ipsilateral to movement) motor cortex. Each of these figures represents the difference in optical absorption between a sample data set and a reference data set. Each sample set is the mean of a specific 5 s long data bin recorded during the movement task. The reference set was taken as the mean of the 20 s of data recorded prior to movement onset. All of these data are grand means over all 15 periods of the movement task.

As one would expect, the greatest increase in optical absorption occurs over the motor cortex contralateral to the hand performing the movement task, and in this case is most evident between C3 and Cp1 at 10–15 s after the start of the stimulus. Such an increase in absorption is characteristic of an increase in cerebral blood flow due to functional activation of the surrounding cortex (Obrig and Villringer 2003). Figure 5B(e) also shows evidence of a lesser ipsilateral motor cortex activation towards the very end of the 30 s period of stimulation while figures 5B(b–e) show only source noise. Some ipsilateral activation is not uncommon in the studies of functional activation of the motor cortex (Franceschini *et al* 2003) and its significance is difficult to establish within a single-subject study.

Figure 6 shows a Bereitschaftspotential recorded at the uppermost electrode over the motor cortex contralateral to the paced, voluntary movement and the signal recorded at the equivalent ipsilateral electrode. These data are the average of 134 events (after 43 were visually rejected due to movement or other artefacts) which were baseline corrected using the period –3.5 to –3 s post-movement. The characteristic slow-building negative deflection, beginning 2 s prior to movement is very apparent over the contralateral electrode (which is at approximately C1) but unexpectedly is not apparent over the ipsilateral electrode (approximately C2) which shows only the typical post-movement positive deflection. The division between early and late BP is not well defined in the data presented here but this is not unusual given the level of noise associated with single-subject event-related potentials (Shibasaki and Hallett 2006).

5. Discussion

We have presented evidence that the opto-electrode probe design described above can be successfully applied in order to obtain near-infrared optical images of cortical haemodynamics and an electroencephalogram simultaneously. The probe is versatile, inexpensive and no more difficult to apply than a standard clinical EEG electrode. It also has the significant advantage of collocating the electrode and the optical fibre, which allows for direct comparison and optimal co-registration of the two sets of data.

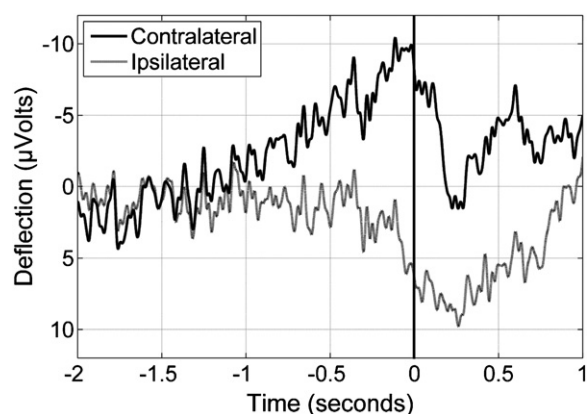


Figure 6. The Bereitschaftspotential recorded at the uppermost electrode over the contralateral (electrode 1) and ipsilateral (electrode 8) motor cortices.

The potential applications of simultaneous NIR imaging and EEG are many and varied. Some notable research has already been undertaken which exploits simultaneous NIR optical and EEG recording in the study of epilepsy (Gallagher *et al* 2008, Roche-Labarbe *et al* 2008). In the near future, we will use the design described here to investigate the relationship between the electrophysiology and haemodynamics of neonatal seizure by applying a combined OT and EEG system at the cot side. We also hope to build on previous studies of haemodynamics (Minagawa-Kawai *et al* 2008) and electrophysiology (Fonteneau and van der Lely 2008) to study language development and specific forms of language impairment in infants and children.

Acknowledgment

We would like to thank Stewart Boyd of the Clinical Neurophysiology Department of Great Ormond Street Hospital for his excellent advice and the loan of the Telefactor and Neuroscan EEG systems. This work has been funded in part by the EPSRC.

References

- Arridge S R 1999 Optical tomography in medical imaging *Inverse Problems* **15** R41–93
- Babiloni C, Carducci F, Cincotti F, Rossini P M, Neuper C, Pfurtscheller G and Babiloni F 1999 Human movement-related potentials vs desynchronization of EEG alpha rhythm: a high-resolution EEG study *NeuroImage* **10** 658–65
- Connolly J F, D'Arcy R C, Lynn Newman R and Kemps R 2000 The application of cognitive event-related brain potentials (ERPs) in language-impaired individuals: review and case studies *Int. J. Psychophysiol.* **38** 55–70
- Everdell N L, Gibson A P, Tullis I D C, Vaithianathan T, Hebden J C and Delpy D T 2005 A frequency multiplexed near-infrared topography system for imaging functional activation in the brain *Rev. Sci. Instrum.* **76** 093705–5
- Flock S T, Jacques S L, Wilson B C, Star W M and van Gemert M J C 1992 Optical properties of intralipid: a phantom medium for light propagation studies *Lasers Surg. Med.* **12** 510–9
- Fonteneau E and van der Lely H K J 2008 Electrical brain responses in language-impaired children reveal grammar-specific deficits *PLoS ONE* **3** e1832
- Franceschini M A, Fantini S, Thompson J H, Culver J P and Boas D A 2003 Hemodynamic evoked response of the sensorimotor cortex measured noninvasively with near-infrared optical imaging *Psychophysiology* **40** 548–60
- Gallagher A *et al* 2008 Non-invasive pre-surgical investigation of a 10 year-old epileptic boy using simultaneous EEG-NIRS *Seizure* **17** 576–82

- Gibson A P, Austin T, Everdell N L, Schweiger M, Arridge S R, Meek J H, Wyatt J S, Delpy D T and Hebden J C 2006 Three-dimensional whole-head optical tomography of passive motor evoked responses in the neonate *NeuroImage* **30** 521–8
- Gibson A P, Hebden J C and Arridge S R 2005 Recent advances in diffuse optical imaging *Phys. Med. Biol.* **50** R1–43
- Gonzalez C, Fan S, Luck S J and Hillyard S A 1994 Sources of attention-sensitive visual event-related potentials *Brain Topogr.* **7** 41–51
- Hillman E M C 2007 Optical brain imaging *in vivo*: techniques and applications from animal to man *J. Biomed. Opt.* **12** 051402
- Hillyard S A and Anillo-Vento L 1998 Event-related brain potentials in the study of visual selective attention *Proc. Natl. Acad. Sci.* **95** 781–7
- Maki A, Yamashita Y, Watanabe E and Koizumi H 1996 Visualizing human motor activity by using non-invasive optical topography *Front. Med. Biol. Eng.* **7** 285–97
- Michel C M, Murray M M, Lantz G, Gonzalez S, Spinelli L and Grave dePeralta R 2004 EEG source imaging *Clin. Neurophysiol.* **115** 2195–222
- Mima T, Sadato N, Yazawa S, Hanakawa T, Fukuyama H, Yonekura Y and Shibasaki H 1999 Brain structures related to active and passive finger movements in man *Brain* **122** 1989–97
- Minagawa-Kawai Y, Dupoux E and Hebden J C 2008 Optical imaging of infants' neurocognitive development: recent advances and perspectives *Dev. Neurobiol.* **68** 712–28
- Mulert C, Jager L, Schmitt R, Bussfeld P, Pogarell O, Moller H-J, Juckel G and Hegerl U 2004 Integration of fMRI and simultaneous EEG: towards a comprehensive understanding of localization and time-course of brain activity in target detection *NeuroImage* **22** 83–94
- Nuwer M 1997 Assessment of digital EEG, quantitative EEG, and EEG brain mapping. Report of the American Academy of Neurology and the American Clinical Neurophysiology Society *Neurology* **49** 277–92
- Obrig H and Villringer A 2003 Beyond the visible—imaging the human brain with light *J. Cereb. Blood Flow Metab.* **23** 1–18
- Peña M, Maki A, Kovačić D, Dehaene-Lambertz G, Koizumi H, Bouquet F and Mehler J 2003 Sounds and silence: an optical topography study of language recognition at birth *Proc. Natl. Acad. Sci. USA.* **100** 11702–5
- Ritter P and Villringer A 2006 Simultaneous EEG-fMRI *Neurosci. Biobehav. Rev.* **30** 823–38
- Roche-Labarbe N, Wallois F, Ponchel E, Kongolo G and Grebe R 2007 Coupled oxygenation oscillation measured by NIRS and intermittent cerebral activation on EEG in premature infants *NeuroImage* **36** 718–27
- Roche-Labarbe N, Zaaimi B, Berquin P, Nehlig A, Grebe R and Wallois F 2008 NIRS-measured oxy- and deoxyhemoglobin changes associated with EEG spike-and-wave discharges in children *Epilepsia* **49** 1871–80
- Rovati L, Salvatori G, Bulf L and Fonda S 2007 Optical and electrical recording of neural activity evoked by graded contrast visual stimulus *BioMed. Eng. Online* **6** 28
- Shibasaki Hiroshi 2008 Human brain mapping: hemodynamic response and electrophysiology *Clin. Neurophysiol.* **119** 731–43
- Shibasaki H and Hallett M 2006 What is the Bereitschaftspotential? *Clin. Neurophysiol.* **117** 2341–56
- Tidswell T, Gibson A, Bayford R H and Holder D S 2001 Three-dimensional electrical impedance tomography of human brain activity *NeuroImage* **13** 283–94
- Zeff B W, White B R, Dehghani H, Schlaggar B L and Culver J P 2007 Retinotopic mapping of adult human visual cortex with high-density diffuse optical tomography *Proc. Natl. Acad. Sci.* **104** 12169–74